J Therm Anal Calorim (2015) 122:339–347
DOI 10.1007/s10973-015-4673-2

Synthesis, thermal study and some properties of Gd(III), Tb(III), Dy(III) and Er(III) complexes with 4,4′-bipyridine and dibromoacetates

A. Czylkowska[1]

Received: 19 November 2014 / Accepted: 25 March 2015 / Published online: 16 April 2015

Abstract New complexes with formulae: Ln(4-bpy)($CBr_2HCOO)_3 \cdot 3H_2O$ (where Ln(III) = Gd, Tb, Dy) and $Er(4\text{-bpy})_{1.5}(CBr_2HCOO)_3 \cdot 3H_2O$, were prepared and characterized by chemical, elemental analysis and IR spectroscopy. The nature of metal–ligand coordination was studied. All of them are crystalline. Gd(III), Tb(III) and Dy(III) complexes are isostructural in one group. Conductivity studies (in methanol, dimethyloformamide and dimethylsulfoxide) were also discussed. The thermal properties of complexes in the solid state were studied using TG–DTG techniques under dynamic flowing air atmosphere. TG–MS system was used for Tb(III) (as an example of isostructural compound) and Er(III) complexes to analyze principal volatile thermal decomposition and fragmentation products evolved during pyrolysis in dynamic flowing air atmosphere.

Keywords Heavy lanthanide complexes · 4,4′-Bipyridine · Dibromoacetates · TG–DTG · TG–MS · IR spectra

Introduction

Lanthanide compounds including N and O donors, as bipyridine isomers and carboxylate groups, are still the subject of current research. Based on the trend of lanthanides to create high coordination numbers and possibility of different coordination of selected organic ligands, it may be stated that such complexes can create a new class of compounds with potentially different functions and application. The mixed halogeno-bipyridine complexes of lanthanide(III) have been the subject of investigation for several years. The nature of bonds between Ln(III) ions and halogenoacetate ligand and bipyridine isomers is discussed in several papers [1–5]. These mixed ligand complexes are of interest because of possibility of various ways of coordination bipyridine and halogenoacetate ligands. These ligands are able to exist as mono- and multidentate donors in metal complexes [1–5]. In the literature [1, 2], there are described compounds, where there is only one type of coordination of carboxylate ligands. The papers [3–10] are examples to occur different possibilities of binding COO groups in one compound.

It is interesting to compare the properties of the mixed ligand lanthanide(III) complexes with 4,4′-bipyridine and chloro- or bromoacetates. These researches are recently undertaken in our laboratory.

Previously, the synthesis and characterization of lanthanide(III) complexes (where Ln(III) = Y, La → Lu without Pm(III)) with 4,4′-bipyridine and di- or trichloroacetates were reported [6–14]. This paper presents the results of new lanthanide complexes with title ligands. It is a continuation of our study on preparation, type of coordination organic ligands and thermal behavior of $Y(4\text{-bpy})_{1.5}(CBr_2HCOO)_3 \cdot 3H_2O$, $Ln(4\text{-bpy})(CBr_2HCOO)_3 \cdot nH_2O$ where Ln(III) = La, Ce, Eu and $Ln(4\text{-bpy})_{0.5}(CBr_2HCOO)_3 \cdot 2H_2O$ where Ln(III) = Pr, Nd, Sm complexes [14, 15].

Experimental

Materials, synthesis and analysis

4,4′-Bipyridine, CBr_2HCOOH, Ln_2O_3 (where Ln(III) = Gd, Dy), Tb_4O_7, Er_2O_3, dimethylsulfoxide (DMSO),

✉ A. Czylkowska
agnieszka.czylkowska@p.lodz.pl

[1] Institute of General and Ecological Chemistry, Lodz University of Technology, Lodz, Poland

Table 1 Analytical data and molar conductivity in MeOH, DMF and DMSO for investigated complexes

Compound	Analysis: found (calculated) (%)				Λ_M (Ω^{-1} cm^2 mol^{-1}); $c = 1 \times 10^{-3}$ mol dm^{-3}		
	Ln	C	N	H	MeOH	DMF	DMSO
$Gd(4\text{-bpy})(CBr_2HCOO)_3{\cdot}3H_2O$	15.55 (15.45)	18.90 (18.88)	2.82 (2.75	1.67 (1.68)	55.0	49.1	52.0
$Tb(4\text{-bpy})(CBr_2HCOO)_3{\cdot}3H_2O$	16.03 (15.58)	18.88 (18.85)	2.81 (2.75)	1.67 (1.68)	52.2	48.8	54.3
$Dy(4\text{-bpy})(CBr_2HCOO)_3{\cdot}3H_2O$	15.96 (15.88)	18.82 (18.78)	2.80 (2.74)	1.69 (1.67)	54.4	46.2	53.0
$Er(4\text{-bpy})_{1.5}(CBr_2HCOO)_3{\cdot}3H_2O$	15.15 (15.12)	22.74 (22.80)	3.74 (3.80)	1.90 (1.91)	51.0	42.5	50.0

dimethylformamide (DMF) and methanol (MeOH) (anhydrous) p.a. were obtained from Aldrich and Lab-Scan, respectively. Water solutions of metal(III) dibromoacetates were prepared by adding 2 mol dm^{-3} dibromoacetic acid to freshly precipitated hydroxides in ca. stoichiometric quantities (in temperature $\leq$18 °C, because lanthanide dibromoacetate solutions are relatively unstable; in the presence of 4-bpy these stability increased).

The mixed ligand complexes were synthesized in the same way as we described in [15]. The contents of metal(III) ions in obtained solutions were mineralized and determined by EDTA titration.

The carbon, hydrogen and nitrogen contents in the prepared complexes were determined by a Carlo-Erba analyzer with V_2O_5 as an oxidizing agent.

Methods and instruments

The X-ray powder diffraction patterns of synthesized complexes and final solid decomposition products in air were recorded on D-5000 diffractometer using Ni-filtered CuK_α radiation. The measurements were taken in the range of 2θ angles 2°–80°. Obtained results were analyzed using the Powder Diffraction File [16]. Molar conductance was measured on a conductivity meter of the OK-102/1 type equipped with an OK-902 electrode at 25 ± 0.5 °C, using 1×10^{-3} mol dm^{-3} solutions of complexes in methanol, dimethylformamide and dimethylsulfoxide. IR spectra were recorded with a NICOLET 6700 Spectrometer (4000–400 cm^{-1} with accuracy of recording 1 cm^{-1}) using KBr pellets. The thermal properties of complexes in air were studied by TG–DTG techniques in the range of temperature 25–1000 °C at a heating rate of 10 °C min^{-1}; TG and DTG curves were recorded on Netzsch TG 209 apparatus in flowing dynamic air atmosphere $v = 20$ cm^3 min^{-1} using ceramic crucibles. The solid intermediate products of pyrolysis in air were determined from TG and DTG curves and confirmed by recording the IR spectra of sinters (prepared during heating the sample of complex up to appropriate temperature defined from the TG or DTG curves). The IR spectra of sinters were analyzed in the region characteristic for 4,4′-bipyridine and dibromoacetates absorption. Additionally, in the sinters, the presence of anions Br^- was also investigated. The TG–MS coupled measurements have been carried out only for Tb(III) and Er(III) complexes using the SETSYS 16/18 apparatus coupled with QMS-422 Balzers spectrometer, in the range of temperature 25–1000 °C at a heating rate 10 °C min^{-1} in flowing air atmosphere $v = 20$ cm^3 min^{-1} in ceramic crucibles. The *m/z* values are given based on ^{1}H, ^{12}C, ^{14}N, ^{16}O and ^{80}Br (additionally ^{13}C and ^{18}O in case of CO_2).

Results and discussion

Table 1 presents results of the elemental and chemical analysis of investigated compounds. They are stable in air in solid state. The analysis of the power diffraction patterns of these compounds reveals that they are crystalline. Gd(III), Tb(III) and Dy(III) complexes are isostructural in one group (Fig. 1). The Er(III) compound is not isostructural with them. There are no powder diffraction patterns of reported complexes in Powder Diffraction File [16]. There were isolated monocrystals of Dy(III) compound, but they have very poor quality (not suitable data for publication). Also in Table 1, there are molar conductivity values for all complexes in solutions of MeOH, DMF and DMSO. All complexes in MeOH and DMF display behaviors intermediate between those of nonelectrolytes and 1:1 electrolytes. In DMSO they are electrolyte type 1:1 [17]. In series of light lanthanide complexes (Ce(III) → Eu(III)) with 4-bpy and dibromoacetates, the molar conductivities in solutions MeOH, DMF and DMSO have similar values. Relative not high molar conductance in MeOH and DMF is characteristic for all complexes compared. The conductivity data suggest that dibromoacetate ligands in obtained compounds are only partially displaced by solvent molecules [18, 19].

IR spectra

In Tables 2 and 3, there are absorption bands in the region characteristic for dibromoacetates and 4-bpy. These spectra are very similar. For all compounds, the ν_{as}(COO)

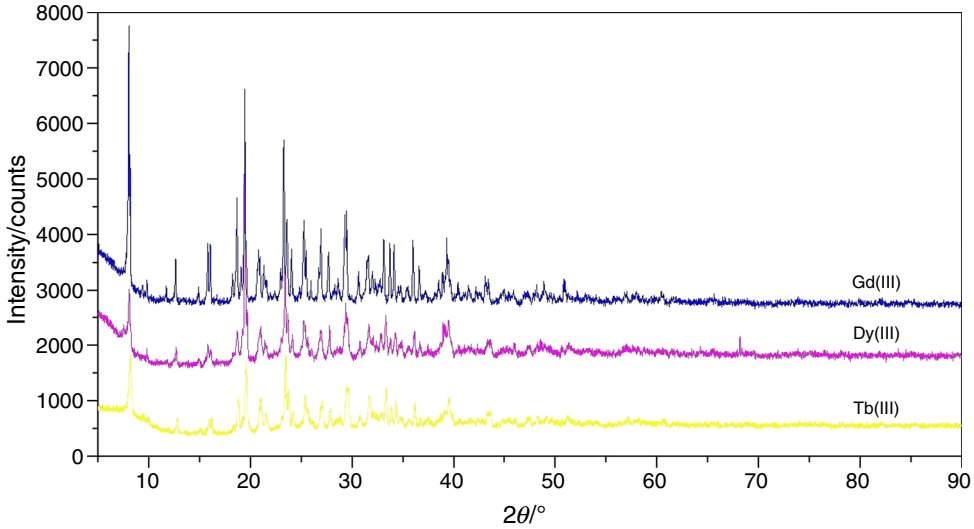

Fig. 1 X-ray diffraction patterns for complexes Ln(4-bpy)$(CBr_2HCOO)_3 \cdot 3H_2O$ (Ln(III) = Gd, Tb, Dy)

Table 2 IR bands of CBr_2HCOO^- groups in $CBr_2HCOONa$ and obtained complexes

$CBr_2HCOONa$ [20]	Complexes				Assignments
	Gd(III)	Tb(III)	Dy(III)	Er(III)	
3015	2985	2985	2985	3022	ν(CH)
1616	1708	1710	1712	1690	ν_{as}(COO)
1378	1389	1388	1390	1412, 1385	ν_s(COO)
1191	1186	1186	1186	1181	ν(CH)
1148	1145	1140	1141	1145	δ(CCOO)
931	950	950	950	950	ν(CC)
698	720	720	720	700	$\nu_s(CBr_2)$

vibration is identified as the strong band in the range 1712–1690 cm^{-1}. The band assigned to the vibration of ν_s(COO) is observed in the range 1412–1385 cm^{-1}. Only for Er(III) complex, ν_s(COO) vibrations are split into two. The vibrations of ν_{as}(COO) and ν_s(COO) are shifted to higher wave numbers. This fact may indicate that the carboxylate groups are bonded to metal(III) ions as bridging ligands [22–24]. For Er(III) compound, probably bridging non-completely equivalent bonds between Er(III) and carboxylate groups exists [25]. In the absorption region of $CBr_2HCOONa$ appear also the stretching modes $\nu_s(CBr_2)$ and δ(CCOO). They are in complexes observed in the ranges: 700–720 cm^{-1} and between 1145 and 1140 cm^{-1}, respectively. The absorption bands of ν(CH) are in the sodium salt at 3015 and 1191 cm^{-1}; in the complexes, they are in the ranges: 3022–2986 and 1181–1186 cm^{-1}.

In the IR spectra of complexes, there are also vibrations of 4-bpy. They are given in Table 3. The observations were made for 4-bpy absorption in the region 4000–600 cm^{-1}. The characteristic band attributed to ν(CC), ν(CN), $\nu(CC_{ir})$ vibrations (symmetry A_1) in pure 4-bpy is at 1588 cm^{-1}, but in complexes, it is in the range 1615–1599 cm^{-1}. The band in the free ligand at 1530 cm^{-1} assigned to ν(CC), ν(CC) vibrations (symmetry B_1) in the IR spectra of complexes, is slightly shifted to higher frequency. The band characteristic for "breathing" mode is moved to higher wave numbers (1003–1000 cm^{-1}) in comparison with free ligand (988 cm^{-1}). Most of aromatic ring deformation bands in plane γ(CH) and out plane β(CH) shift to lower and higher frequency after coordination with metal ion [21].

In addition, a broad band in the water stretching region (ca 3450–3350 cm^{-1}) appears for all complexes described.

Thermal decomposition in air

The TG–DTG methods were used to describe thermal decomposition in air of synthesized complexes. First step of pyrolysis is dehydration. After that, partial decomposition and next total decomposition of organic ligands take place. Most processes are poorly separated from each other. In several intermediate solid products, presence of bromide, carboxylate group and bipyridine was identified. As a final,

Table 3 IR bands for free 4-bpy and 4-bpy in obtained complexes

4-bpy [21]	Complexes				Assignments
	Gd(III)	Tb(III)	Dy(III)	Er(III)	
1588	1610	1600	1615	1599	υ(CC), υ(CN), $\upsilon(CC_{ir})$, A_1
1530	1535	1532	1531	1535	υ(CC), υ(CN) B_1
1488	1490	1487	1490	1498	υ(CC), υ(CN)
1403	1403	1404	1405	1403	υ(CC), υ(CN)
1328	1320	1320	1320	1320	υ(CC), υ(CN)
1205	1210	1205	1205	1219	β(CH)
1092	–	–	–	–	β(CH)
1072	1065	1066	1065	1066	β(CH)
1037	1045	1045	1045	1043	"Ring breathing"
988	1000	1001	1000	1003	"Ring breathing"
962	*	*	*	970	γ(CH)
850	850	850	850	830	γ(CH)
810	806	806	806	805	γ(CH)
745	790	789	790	–	γ(CH)
733	735	733	733	730	γ(CH)
672	680	679	680	683	γ(CH)
608	620	619	620	623	β(CH)

ir—inter ring bands; A_1—symmetry A_1, B_1—symmetry B_1

* overlap by dibromoacetates absorption

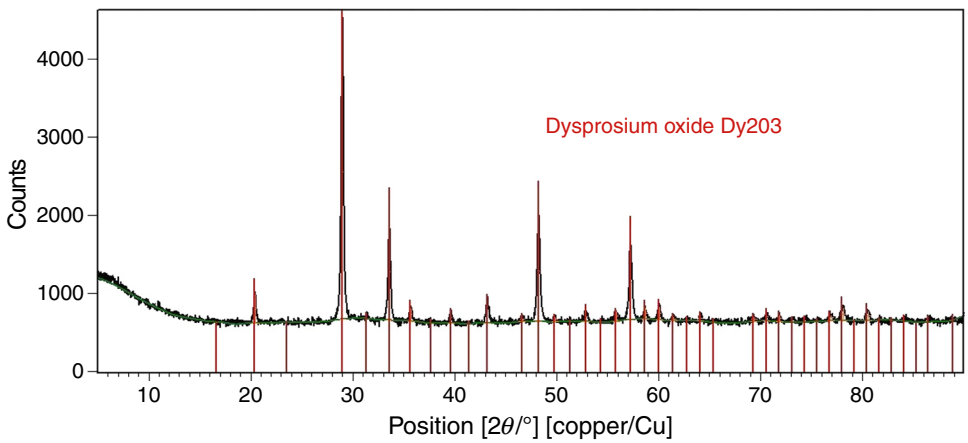

Fig. 2 X-ray diffraction patterns for sinter of Dy(III) complex at 800 °C (pure Dy_2O_3)

solid decomposition products are suitable lanthanide oxides. This has been proven on the basis of diffraction patterns (as an example Fig. 2) taken for final solid products. All synthesized compounds do not reveal the effect of creating LnOBr. Figures 3, 4, 5 6 show profiles of TG and DTG of all obtained complexes. Results of thermal analysis are presented in Table 4.

$Gd(4\text{-bpy})(CBr_2HCOO)_3{\cdot}3H_2O$ starts to decompose at 75 °C. In the temperature ranges: 75°–100° and 100–200 °C, two-stage dehydration takes place. First, Gd(III) complex loses one water molecule and next two moles of water. Anhydrous compound is stable up to 200 °C. When temperature rises, partial decomposition of dibromoacetates occurs. Probably intermediate solid product appears, $Gd(4\text{-bpy})(CBr_2HCOO)_{2.75}{\cdot}Br_{0.25}$ (mass lose calculated 3.67 % and found 4.0 %). On DTG curve appears peak at 205 °C. Next (220–290 °C), there is further decomposition of halogenoacetates probably via $Gd(4\text{-bpy})(CBr_2HCOO){\cdot}Br_2$ accompanied with strong maximum on DTG at 245 °C. Subsequent thermolysis of $Gd(4\text{-bpy})(CBr_2HCOO){\cdot}Br_2$ is observed with DTG peaks at 330, 440 and 815 °C. Horizontal mass level for Gd_2O_3 begins at 835 °C.

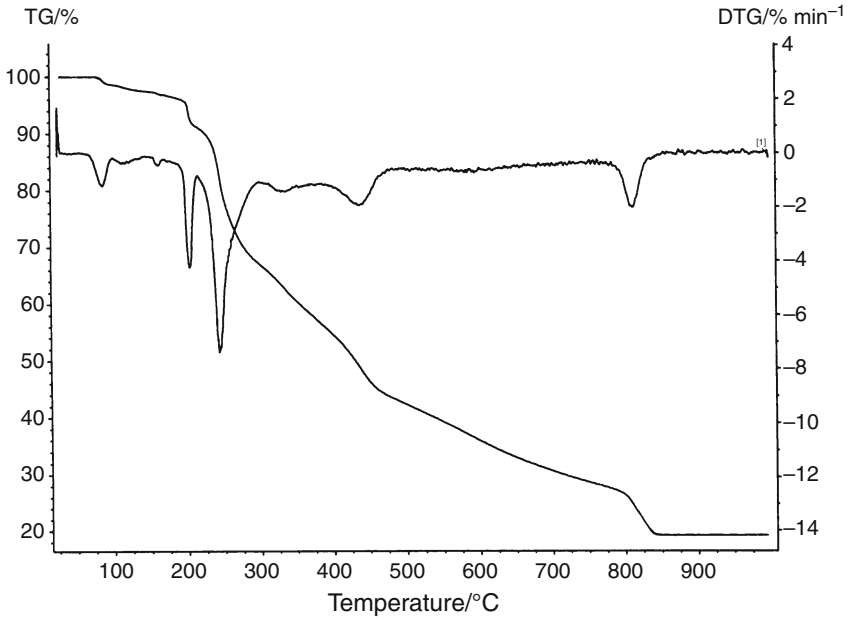

Fig. 3 TG and DTG curves of thermal decomposition of $Gd(4\text{-bpy})(CBr_2HCOO)_3{\cdot}3H_2O$ recorded in air atmosphere; mass sample 6.32 mg

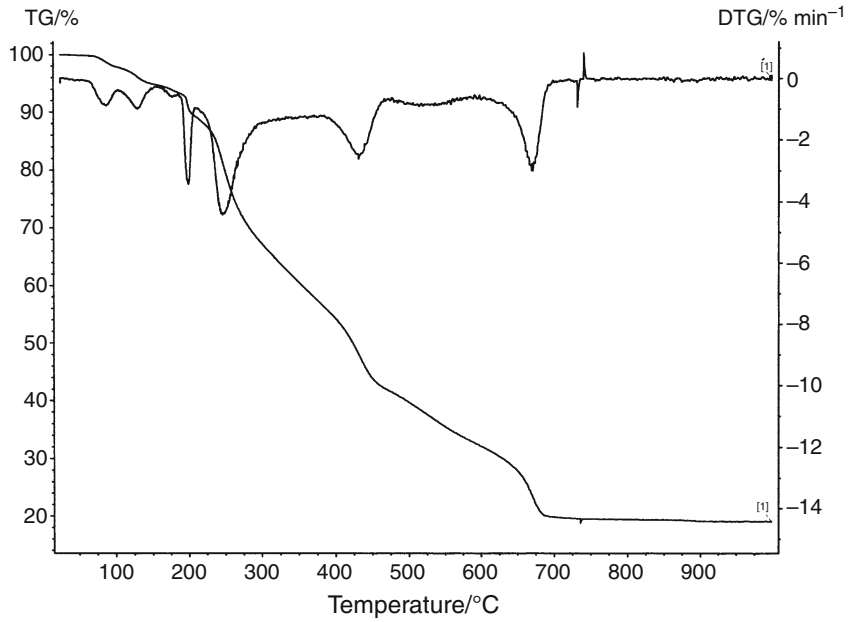

Fig. 4 TG and DTG curves of thermal decomposition of $Tb(4\text{-bpy})(CBr_2HCOO)_3{\cdot}3H_2O$ recorded in air atmosphere; mass sample 8.90 mg

Terbium(III) complex decomposes, also as Gd(III) compound, at 75 °C. First, it loses one and next two molecules of water. On DTG curve, there are two peaks at 80 and 135 °C. Above 155 °C, $Tb(4\text{-bpy})(CBr_2HCOO)_3$ converts probably to $Tb(4\text{-bpy})(CBr_2HCOO)_{2.5}{\cdot}Br_{0.5}$. It is accompanied with DTG peak at 200 °C. Further heating causes decomposition of first partial and then total organic ligands (DTG maximum at 245, 430 and 660 °C). These processes are poorly separated from each other. A plateau on TG curve for Tb_4O_7 begins above 750 °C (mass lose calculated 81.67 % and found 81.3 %).

Dy(III) compound is stable up to 60 °C. On the beginning, complex loses 1.5 mol of water. In the range of temperature 125–200 °C further dehydration and decomposition to $Dy(4\text{-bpy})(CBr_2HCOO)_{2.75}{\cdot}Br_{0.25}$ take place (mass lose calculated 5.99 % and found 6.0 %). This is connected with DTG peak at 185 °C. Next (200–350 °C), $Dy(4\text{-bpy})(CBr_2HCOO)_{0.5}{\cdot}Br_{2.5}$ appears. After that, further pyrolysis (destruction of dibromoacetate groups and oxidation of organic fragments) takes place by the overlap of multiple processes. The DTG curve shows peaks at 250° (with shoulder at 260°), 430 and 770 °C. At 800 °C, Dy_2O_3 forms.

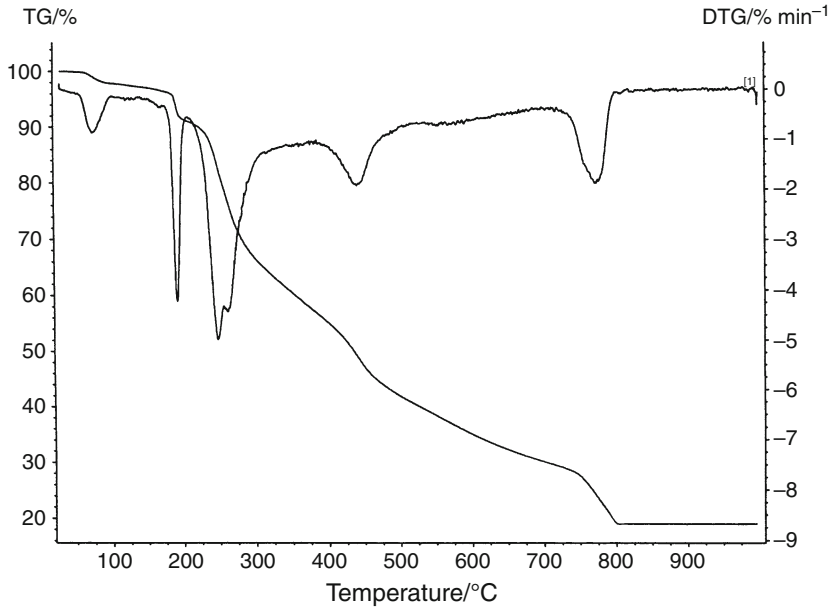

Fig. 5 TG and DTG curves of thermal decomposition of $Dy(4\text{-bpy})(CBr_2HCOO)_3{\cdot}3H_2O$ recorded in air atmosphere; mass sample 9.96 mg

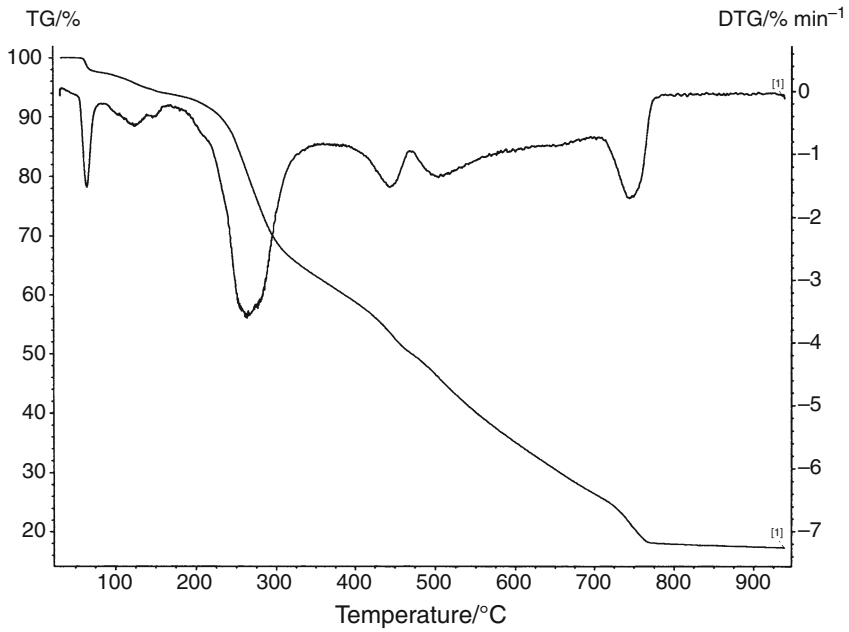

Fig. 6 TG and DTG curves of thermal decomposition of $Er(4\text{-bpy})_{1.5}(CBr_2HCOO)_3{\cdot}3H_2O$ recorded in air atmosphere; mass sample 10.36 mg

Er(III) complex is stable up to 50 °C. Dehydration process occurs in two steps. Above 50 °C, one and half water molecules are lost (50–80 °C). The second step takes place between 80 and 145 °C. It is connected with leaving the remaining water. On DTG curve, there are peaks at 65° and 125° with shoulder at 150 °C. With increasing temperature is partial and total destroying of organic ligands probably via $Er(4\text{-bpy})_{1.5}(CBr_2HCOO)_{0.5}{\cdot}Br_{2.5}$. Above 775 °C, pure Er_2O_3 appears.

TG–MS study for Tb(III) and Er(III) complexes in air

Moreover, TG–MS system was used to analyze the principal volatile products evolved during thermal decomposition and fragmentation in dynamic air atmosphere. TG–MS study was made only for terbium(III) (as a representative of isostructural compounds) and erbium(III) complexes. The detection of volatile species and fragmentation

Table 4 Thermal decomposition data for obtained complexes in air atmosphere

Complex	Temperature range/°C	Principal peaks of DTG temperature/°C	Mass loss/%		Intermediate and final solid products
			Calc.	Found.	
$Gd(4\text{-bpy})(CBr_2HCOO)_3\cdot 3H_2O$	75–100	80	1.77	1.8	$Gd(4\text{-bpy})(CBr_2HCOO)_3\cdot 2H_2O$
	100–200	160	3.54	3.2	$Gd(4\text{-bpy})(CBr_2HCOO)_3$
	200–220	205	3.67	4.0	$Gd(4\text{-bpy})(CBr_2HCOO)_{2.75}Br_{0.25}$[b]
	220–290	245	23.23	23.0	$Gd(4\text{-bpy})(CBr_2HCOO)Br_2$[a]
	290–835	330, 440, 815	49.99	49.5	Gd_2O_3
$Tb(4\text{-bpy})(CBr_2HCOO)_3\cdot 3H_2O$	75–100	80	1.77	1.80	$Tb(4\text{-bpy})(CBr_2HCOO)_3\cdot 2H_2O$
	100–155	135	3.54	3.5	$Tb(4\text{-bpy})(CBr_2HCOO)_3$
	155–220	200	6.70	6.5	$Tb(4\text{-bpy})(CBr_2HCOO)_{2.5}Br_{0.5}$[b]
	220–290	245	20.11	20.0	$Tb(4\text{-bpy})(CBr_2HCOO)Br_2$[a]
	290–750	430, 660	49.55	49.5	Tb_4O_7
$Dy(4\text{-bpy})(CBr_2HCOO)_3\cdot 3H_2O$	60–125	75	2.64	2.5	$Dy(4\text{-bpy})(CBr_2HCOO)_3\cdot 1.5H_2O$
	125–200	185	5.99	6.0	$Dy(4\text{-bpy})(CBr_2HCOO)_{2.75}Br_{0.25}$[b]
	200–350	250, 260sh	30.11	30.0	$Dy(4\text{-bpy})(CBr_2HCOO)_{0.5}Br_{2.5}$[a]
	350–800	430, 770	43.04	43.0	Dy_2O_3
$Er(4\text{-bpy})_{1.5}(CBr_2HCOO)_3\cdot 3H_2O$	50–80	65	2.44	2.5	$Er(4\text{-bpy})_{1.5}(CBr_2HCOO)_3\cdot 1.5H_2O$
	80–145	125, 150sh	2.44	2.5	$Er(4\text{-bpy})_{1.5}(CBr_2HCOO)_3$
	145–340	260	30.96	31.0	$Er(4\text{-bpy})_{1.5}(CBr_2HCOO)_{0.5}Br_{2.5}$[a,b]
	340–775	440, 500, 745	46.87	46.0	Er_2O_3

sh shoulder

[a] Projected by DTG curve on TG curve

[b] In the sinters of several solid intermediate products, bromide anions and IR bands' characteristic for carboxylate groups and 4,4′-bipyridine were identified

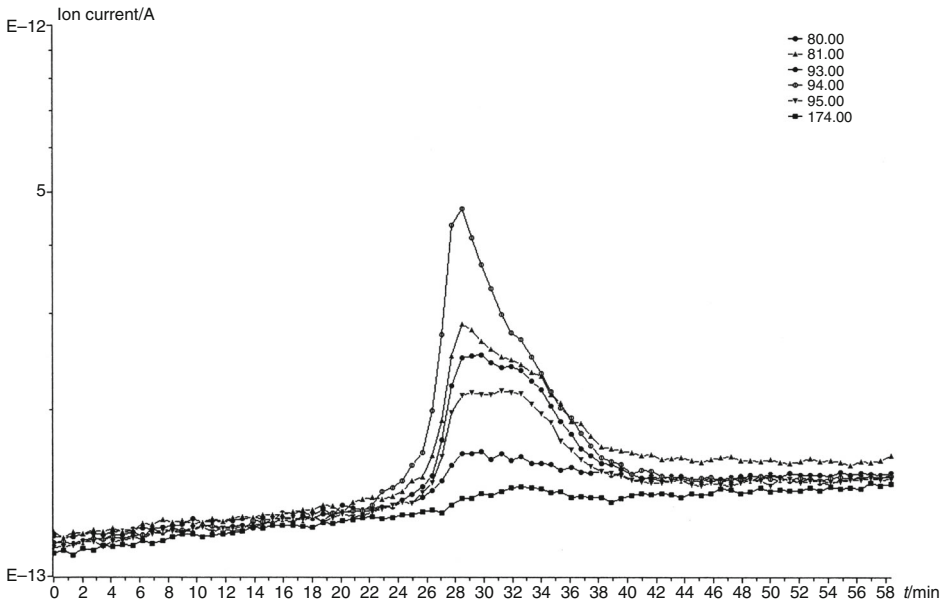

Fig. 7 Ion current vs time for terbium(III) complex of volatile products contain bromine atom; mass sample 10.80 mg

in appropriate temperature range (270–370 °C for Tb(IIII) and 260–360 °C in case of Er(III)) correspond exactly to the sudden mass loss presented in Table 4. Major maxima for ion current are for Tb(III) at: 270, 450 and 680 °C. In case of Er(III) compound, they are at: 265, 455, 514 and 720 °C. The peak characteristic for OH^+, H_2O^+ ($m/z = 17$, 18) appears as a broad maximum in the temperature range 90–320 °C. It connects with dehydration and partial

decomposition dibromoacetate ligands. For terbium(III) complex, the profiles of C^+ and CO_2^+ (m/z = 12, 44, 45, 46) are maximum at 180° and 233°, and with very high intensity at 280, 460, 517 and 694 °C. In case of the erbium(III) compound, they are at: 146° (with low intensity), 270, 455, 515 and 720 °C. For investigated complexes, the bromide species corresponding to $m/z = 80$ (Br^+), 81 (HBr^+), 93 ($CHBr^+$), 94 (CH_2Br^+), 95 (CH_3Br^+), 174 ($CH_2Br_2^+$) are in the temperature range 250–400 °C. It is associated with destruction of dibromoacetates. There are also fragments $m/z = 15$ (CH_3^+ or NH^+) and 30 (CH_2O^+ or NO^+). Maximum formation of CH_3^+ or NH^+ is at 280 °C. Evolution of CH_2O^+ or NO^+ is at 670 °C (Tb(III)) and 725 °C (Er(III)). The mass spectrometer detected also traces of other ion signals. Figure 7 presents hemogram of Tb(III) complex consisting of only principal bromide species versus time.

Conclusions

1. In this paper, there is information about obtained complexes of Gd(III), Tb(III), Dy(III) and Er(III) with empirical formulae: $Ln(4\text{-bpy})(CBr_2HCOO)_3{\cdot}3H_2O$ (where Ln(III) = Gd, Tb, Dy) and $Er(4\text{-bpy})_{1.5}(CBr_2HCOO)_3{\cdot}3H_2O$. All compounds were synthesized in the same experimental conditions.
2. The compounds of Gd(III), Tb(III) and Dy(III) are isostructural in one group.
   None of the obtained complexes is isostructural of compounds of Y(III), La(III) → Eu(III) (without Pm(III)) with 4,4′-bipyridine and dibromoacetates [14, 15].
3. The IR spectroscopy data for obtained Gd(III), Tb(III), Dy(III) and Er(III) compounds confirm that the metal ions(III) are bonded with title ligands. The shifts of bands characteristic for ν_{as}(COO) and ν_s(COO) vibrations in complexes correspond to bridging nature of carboxylate groups.
4. During heating in air, all complexes decompose in multistage. Some stages of pyrolysis are weakly separated one from another. Decomposition of investigated compounds begins with total or partial loss of water. Elevation of temperature is connected with partial destruction of ligands containing bromides. The final solid residues are pure oxides.
5. MS data for Tb(III) and Er(III) complexes detected several profiles of ion currents. The principal volatile products evolved during thermal decomposition and fragmentation processes in dynamic air atmosphere are: OH^+, H_2O^+, C^+, CO_2^+, Br^+, HBr^+, $CHBr^+$, CH_2Br^+, CH_3Br^+, $CH_2Br_2^+$, CH_2O^+ or NO^+, CH_3^+ or NH^+.

References

1. Weimin L, Yiqiang C, Nan D, Jianming G, Chenggang C. Synthesis, characterization and crystal structure of diaquadi(2,2′-bipyridine)di(dichloroacetato)lanthanide(III) monodichloroacetato. J Coord Chem. 1994;35:51. doi:10.1080/00958979508033085.
2. Rohde A, John D, Urland W. Crystal structures of $Gd_2(Cl_3CCOO)_6(bipy)_2(H_2O)_2{\cdot}4\text{-bipy}$, $Pr(Cl_3CCOO)_3(bipy)_2$, $Nd(Cl_3CCOO)_3(bipy)_2$ and $Er(Cl_3CCOO)_3(bipy)_2(H_2O)$. Z Kristal. 2005;220(2):177. doi:10.1524/zkri.220.2.177.59141.
3. John D, Urland W. Crystal structure and magnetic behaviour of the new gadolinium complex compound $Gd_2(ClH_2CCOO)_6(bipy)_2$. Eur J Inorg Chem. 2005;22:4486. doi:10.1002/ejic.200500734.
4. Rohde A, Urland J. Catena-Poly[[(2,2′-bipyridine-κ^2N, N′)-praseodymium(III)]-μ-dichloroacetate-1κ^2O:O′:2κO-di-μ-dichloroacetato-κ^4O:O′]. Acta Cryst. 2006;E62:2843. doi:10.1107/S160053680603995X.
5. Rohde A, Urland J. Catena-Poly[[(2,2′-bipyridine-κ^2N, N′)-neodymium(III)]-μ-dichloroacetate-1κ^2O:O′:2κO-di-μ-dichloroacetato-κ^4O:O′]. Acta Cryst. 2006;E62:1618. doi:10.1107/S1600536806022872.
6. Czylkowska A, Kruszynski R, Czakis-Sulikowska D, Markiewicz M. Coordination polymer of lanthanum: synthesis, properties and crystal structure of $[La(4,4'\text{-bipyridine})(CCl_2HCOO)_3(H_2O)]_n$. J Coord Chem. 2007;60(24):2659–69.
7. Kruszyński R, Czylkowska A, Czakis-Sulikowska D. A novel carboxylic coordination polymer of samarium(III): $[Sm(H_2O)(4,4'\text{-bipyridine})(CCl_2HCOO)_3]_n$. J Coord Chem. 2006;59(6):681–90.
8. Czylkowska A, Markiewicz M. Coordination behaviour and thermolysis of some rare-earth complexes with 4,4′-bipyridine and di- or trichloroacetates. J Therm Anal Calorim. 2010;100(2):717–23.
9. Czylkowska A, Czakis-Sulikowska D, Kruszynski R, Markiewicz M. Synthesis, crystal structure and other properties of the complexes of Er(III), Yb(III) and Lu(III) with 4,4′-bipyridine and dichloroacetates. Struct Chem. 2010;21(2):415–23.
10. Czylkowska A, Czakis-Sulikowska D, Kaczmarek A, Markiewicz M. Thermal behavior and other properties of Pr(III), Sm(III), Eu(III), Gd(III), Tb(III) complexes with 4,4′-bipyridine and trichloroacetates. J Therm Anal Calorim. 2011;105(1):331–9.
11. Czakis-Sulikowska D, Czylkowska A, Markiewicz M. Synthesis, characterization and thermal decomposition of yttrium and light lanthanides with 4,4′-bipyridine and dichloroacetates. Polish J Chem. 2007;81(7):1267–75.
12. Czakis-Sulikowska D, Czylkowska A, Markiewicz M, Frajtak M. Synthesis and properties of complexes of Gd(III), Tb(III), Ho(III) and Tm(III) with 4,4′-bipyridine and dichloroacetates. Polish J Chem. 2009;83(11):1893–901.
13. Czylkowska A. New complexes of heavy lanthanides with 4,4′-bipyridine and trichloroacetates. J Therm Anal Calorim. 2011;105(1):331–9.
14. Czylkowska A, Markiewicz M. Synthesis, thermal behavior, and other properties of Y(III) and La(III) complexes with 4,4′-bipyridine and trichloro-or dibromoacetates. J Therm Anal Calorim. 2012;109(2):727–34.
15. Czylkowska A. Synthesis and some properties of light lanthanide complexes with 4,4′-bipyridine and dibromoacetates: thermal study. J Therm Anal Calorim. 2013;114:989.

16. Powder Diffraction File, PDF-2. The International Centre for Diffraction Data (ICDD) 12 Campus Boulevard, Newton Square, PA, USA 2004.
17. Geary WI. The use of conductivity measurements in organic solvents for the characterisation of coordination compounds. Coord Chem Rev. 1971;7:81–122. doi:10.1016/S0010-8545(00)80009-0.
18. Harris CM, McKenzie ED. Nitrogenous chelate complexes of transition metals.III. Bis-chelate complexes of nickel(III) with 1,10-phenantroline, 2,2′-bipyridyl and analogous ligands. J Inorg Nucl Chem. 1967;29(4):1047–68.
19. Feltman RD, Hayter RG. The electrolyte type of ionized complexes. J Chem Soc 1964;4587–91.
20. Spinner E. The vibration spectra of some substituted acetate ions. J Chem Soc 1964;4217.
21. Pearce CK, Grosse DW, Hessel W. Effect of molecular structure on infrared spectra of six isomers of bipyridine. Chem Eng Data. 1970;15:567–70. doi:10.1021/je60047a042.
22. Manhas BS, Trikha AK. Relationships between the direction of shifts in the carbon-oxygen stretching frequencies of carboxylato complexes and the type of carboxylate coordination. Indian J Chem. 1982;59:315–9.
23. Liu J-Y, Ren N, Zhang J-J, He S-M, Wang S-P. Crystal structures, thermal properties, and biological activities of a series of lanthanide compounds with 2,4-dichlorobenzoic acid and 1,10-phenanthroline. Ind Eng Chem Res. 2013;52:6156–63.
24. Zhang Y-Y, Ren N, Xu S-L, Zhang J-J, Zhang D-H. A series of binuclear lanthanide(III) complexes: crystallography, antimicrobial activity and thermochemistry properties studies. J Mol Struct. 2015;1081:413–25.
25. Brzyska W, Ożga W. Spectral, magnetic and thermal investigations of some *d*-electron element 3-methoxy-4-methylbenzoates. J Therm Anal Calorim. 2006;84:385–9. doi:10.1007/s10973-005-6855-9.